Reduced-Order Dynamic Modeling and Stabilizing Control of a Micro-Helicopter

Derek A. Paley* David S. Warshawsky†

Soldier-portable UAVs enhance combat situational awareness by providing an over-the-horizon surveillance platform. This advantage can be multiplied by using multiple micro-helicopters (< 20 g, < 20 cm) that operate cooperatively to obtain synoptic vantage points. Cooperative control of multiple helicopters using theoretically justified control laws requires a mathematical model of micro-helicopter dynamics, which can be quite complex. This paper describes an idealized 3D dynamic model of a micro-helicopter whose control input is the thrust of the main and tail rotors. We use the dynamic model to synthesize tracking-control algorithms for altitude and yaw or altitude and yaw-rate. We further validate the closed-loop model by experimentally demonstrating altitude control of a single helicopter using motion-capture feedback. By leveraging existing results for cooperative control of the closed-loop helicopter model, this paper provides the foundation for the design of a cooperative micro-helicopter surveillance network.

Nomenclature

G	Center of mass of the helicopter
F_1	Main-rotor thrust, N
F_2	Tail-rotor thrust, N
l	Yaw moment arm, m
O	Origin of inertial frame
$\mathbf{r}_{G/O}$	Vector position of G relative to O, m
$\mathbf{v}_{G/O}$	Inertial velocity of G relative to O, m/s
$\mathcal{I}$	Inertial reference frame
$\mathcal{B}$	Body-fixed reference frame
$\mathcal{C}$	Path-based reference frame
r	Horizontal component of position (complex), m
z	Vertical component of position (altitude), m
θ	Yaw angle, rad
ψ	(Horizontal) direction of motion, rad
β	Crab angle, rad
v	Horizontal speed, m/s
z_d	Reference altitude, m
θ_d	Reference yaw angle, rad
u	Reference yaw rate, rad/s

I. Introduction

The U.S. Army's 2004 cancellation of the RAH-66 Comanche helicopter program coincided with the in-theatre emergence of small, soldier-portable autonomous aviation systems. Mixed teaming of manned and unmanned assets is a leading operational paradigm in Iraq and Afghanistan. Soldier-portable unmanned

*Assistant Professor, Department of Aerospace Engineering, University of Maryland, College Park, MD 20742, and AIAA Professional Member.

†Department of Aerospace Engineering, University of Maryland, College Park, MD 20742

(a) Two Silverlit PicooZ RC micro-helicopters

(b) U. Maryland VICON Motion Capture Facility

Figure 1. (a) The Silverlit PicooZ RC micro-helicopter is 17 cm long and weighs 10 grams. Each helicopter is equipped with a set of reflective markers used for motion capture. (b) The VICON Motion Capture Facility in the Autonomous Vehicle Laboratory at the University of Maryland supports (off-board) state-feedback control of autonomous vehicles.

surveillance platforms, like the RQ-11 Raven, provide real-time over-the-horizon viewpoints that dramatically improve situational awareness. The Raven, which weighs four and a half pounds and has a three-foot wingspan, can be operated either remotely or in an autonomous waypoint-navigation mode that uses GPS.

The next generation of Army UAVs will be lighter, smaller, and more capable—following similar trends in commercially available hobby helicopters. For example, the Silverlit PicooZ radio-controlled helicopter shown in Figure 1(a) is 17 cm long and weighs 10 grams. A single solder can carry and launch dozens of these micro-helicopters. However, existing capabilities for remote-control and remote-monitoring of multiple UAVs do not scale well. Next-generation autonomous capabilities will likely include cooperative behavior as well as gust tolerance, building penetration, and target identification and tracking.

Decentralized and cooperative behavior of multiple autonomous surveillance platforms reduces operator workload and elevates situational awareness by providing multiple, coordinated vantage points. A large selection of theoretically justified cooperative control strategies is presently available for a set of UAV models with idealized dynamics. For example, the Dubin's vehicle (a self-propelled particle moving a constant speed subject to a steering control[1]) is an idealized dynamic model that captures the essential elements of a constant-altitude, constant-speed UAV executing a sequence of coordinated turns. Cooperative control of Dubin's vehicles and other simple vehicles models is a well-studied problem.[4,7–11]

The design of cooperative control algorithms for UAVs with complex dynamics, such as micro-helicopters, is mathematically formidable. A powerful design strategy employed in this paper is reduced-order dynamic modeling. We derive from first principles an idealized dynamic model of a micro-helicopter and design its closed-loop dynamics to support the application of existing cooperative control strategies. The helicopter dynamic model is eight-dimensional (its pitch and roll are assumed to be static). We propose separate control algorithms to track a reference altitude and reference yaw angle or yaw-angle rate. The closed-loop helicopter dynamics with altitude-control and yaw-rate-control resembles Dubin's vehicle, and thus provides the foundation for cooperative control of a micro-helicopter fleet. The theoretical analysis is supplemented by numerical simulation and by experimental flight tests conducted in the U. Maryland VICON Motion Capture Facility shown in Figure 1(b).

The paper is organized as follows. In Section II we describe an idealized 3D dynamic model of a micro-helicopter with two control inputs corresponding to the main-rotor and tail-rotor thrust forces. In Section III we use Lyapunov-based methods to propose feedback control algorithms that stabilize to reference values the helicopter's altitude and either yaw or yaw-rate. In Section IV, we describe results from flight tests of altitude control of a PicooZ micro-helicopter with motion-capture based feedback. In Section V we indicate ongoing and future research that support the development of a micro-helicopter surveillance network.

II. Dynamic Model

An idealized 3D dynamic model of a micro-helicopter is shown in Figure 2. The center of mass of the helicopter is denoted by G. Two forces, denoted by F_1 and F_2, act on the helicopter; they represent the

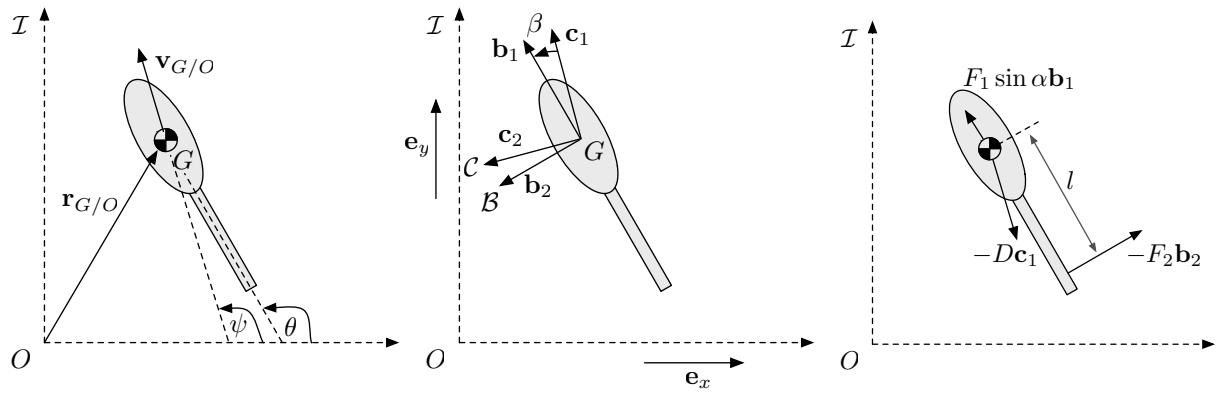

(a) Coordinates (b) Reference frames (c) Free-body diagram

Figure 2. Top-view of 3D micro-helicopter model. The main-rotor thrust, F_1, acts in a direction tilted slightly forward (in the body frame, $\mathcal{B}$) from the vertical by an angle, α. The tail-rotor thrust, F_2, acts horizontally with a yaw moment arm of l about G. (The out-of-plane forces are not shown.)

thrust generated by the main rotor and the thrust generated by the tail rotor, respectively. We assume that the main-rotor thrust acts in a direction tilted slightly forward (in the body frame) from the vertical by an angle, $\alpha > 0$; since we assume that this force acts at the center of mass, it generates no pitch moment.[a] The tail-rotor thrust acts horizontally, with a yaw moment arm of l about G.[b] We assume that the center of mass is coincident with the center of drag so that there is no drag moment. The notation $\mathbf{r}_{G/O}$ denotes the (vector) position of G with respect to an inertially fixed point O; $\mathbf{v}_{G/O}$ and $\mathbf{a}_{G/O}$ denote the inertial velocity and inertial acceleration, respectively, of the center of mass.

We define an inertial frame $\mathcal{I} = (O, \mathbf{e}_x, \mathbf{e}_y, \mathbf{e}_z)$, where O is the origin of the frame and $\mathbf{e}_x$, $\mathbf{e}_y$, and $\mathbf{e}_z$ are orthonormal unit vectors; $\mathcal{B} = (G, \mathbf{b}_1, \mathbf{b}_2, \mathbf{b}_3)$ represents a body frame attached to the helicopter. We assume that $\mathbf{b}_1$ is aligned with the forward axis of the helicopter and that the body-fixed vertical axis, $\mathbf{b}_3$, is permanently aligned with $\mathbf{e}_z$, the inertial vertical axis. We introduce a path frame, $\mathcal{C} = (G, \mathbf{c}_1, \mathbf{c}_2, \mathbf{c}_3)$, such that $\mathbf{c}_1$ is always aligned with the horizontal component of the inertial velocity and $\mathbf{c}_3$ is always aligned with $\mathbf{e}_z$. The frames $\mathcal{I}$, $\mathcal{B}$, and $\mathcal{C}$ are related by the following transformation table (see Figure 2(b)),

	$\mathbf{e}_x$	$\mathbf{e}_y$	$\mathbf{e}_z$	$\mathbf{c}_1$	$\mathbf{c}_2$	$\mathbf{c}_3$
$\mathbf{b}_1$	$-\sin\theta$	$\cos\theta$	0	$\cos\beta$	$\sin\beta$	0
$\mathbf{b}_2$	$-\cos\theta$	$-\sin\theta$	0	$-\sin\beta$	$\cos\beta$	0
$\mathbf{b}_3$	0	0	1	0	0	1,

(1)

where $\beta = \theta - \psi$ represents the crab angle between the body frame and the path frame.

By assuming pitch and roll are constant, we reduce the dimensionality of the configuration space of the rotorcraft dynamic model from twelve to eight. Let x, y, and z denote the Cartesian coordinates of G in $\mathcal{I}$; v is the horizontal speed; ψ (direction of motion) and θ (yaw) are the angular displacements about the vertical axes of the $\mathcal{B}$ and $\mathcal{C}$ frames, respectively. We use a complex number $r = x + iy$ to represent the horizontal position of G; note $v = |\dot{r}|$ and $\psi = \arg(\dot{r})$. The kinematics of the helicopter's center of mass are

$$\mathbf{v}_{G/O} = v\mathbf{c}_1 + \dot{z}\mathbf{c}_3 \tag{2}$$

$$\mathbf{a}_{G/O} = \dot{v}\mathbf{c}_1 + v\dot{\psi}\mathbf{c}_2 + \ddot{z}\mathbf{c}_3. \tag{3}$$

Using the free-body diagram in Figure 2(c) and including the vertical forces, the inertial acceleration of the helicopter's center of mass is

$$\begin{aligned} m\mathbf{a}_{G/O} &= F_1\cos\alpha\mathbf{b}_3 + F_1\sin\alpha\mathbf{b}_1 - D\mathbf{c}_1 - mg\mathbf{b}_3 - F_2\mathbf{b}_2 \\ &= (F_1\sin\alpha - D\cos\beta)\mathbf{b}_1 + (D\sin\beta - F_2)\mathbf{b}_2 + (F_1\cos\alpha - mg)\mathbf{b}_3, \end{aligned} \tag{4}$$

[a]Tilting the main-rotor thrust vector in a PicooZ can be accomplished by adding a small mass to the nose of the helicopter.

[b]The modelled tail-rotor thrust is actually a differential thrust; we assume that there is a baseline tail-rotor thrust that automatically counteracts the rotational momentum of the main-rotor, as is the case with the Silverlit PicooZ.

where $m > 0$ is the mass of the helicopter, g is the acceleration of gravity, and D is the magnitude of the horizontal component of drag. We assume that the horizontal drag has a quadratic dependence on horizontal speed, i.e., $D = \gamma \|\mathbf{v}_{G/O} \cdot \mathbf{c}_1\|^2 = \gamma v^2$, where γ is a drag coefficient. (We ignore the vertical component of drag.) Expressed as components in the path frame, $\mathcal{C}$, the inertial acceleration of G is

$$m\mathbf{a}_{G/O} = (F_1 \sin\alpha\cos\beta + F_2 \sin\beta - \gamma v^2)\mathbf{c}_1 + (F_1 \sin\alpha \sin\beta - F_2\cos\beta)\mathbf{c}_2 + (F_1\cos\alpha - mg)\mathbf{c}_3. \quad (5)$$

The rotational acceleration of the helicopter is governed by

$$I\ddot{\theta}\mathbf{c}_3 = lF_2\mathbf{c}_3, \quad (6)$$

where $I > 0$ is the moment of inertia of the helicopter about the $\mathbf{b}_3$ axis.

Comparing (3) and (5), and using the definition of $\dot{r}$, v, and ψ, we obtain the following equations of motion for the helicopter,

$$\dot{r} = ve^{i\psi} \quad (7)$$

$$\dot{v} = \frac{1}{m}(F_1 \sin\alpha\cos\beta + F_2\sin\beta - \gamma v^2) \quad (8)$$

$$\dot{\psi} = \frac{1}{mv}(F_1\sin\alpha\sin\beta - F_2\cos\beta) \quad (9)$$

$$\ddot{\theta} = \frac{l}{I}F_2 \quad (10)$$

$$\ddot{z} = \frac{1}{m}F_1\cos\alpha - g \quad (11)$$

Note, (7)–(11) represent eight real, first-order differential equations of motion. In the next section, we design the control inputs F_1 and F_2.

III. Stabilizing Controls

In this section, we apply Lyapunov-based design methods to provide separate feedback controls to stabilize the helicopter altitude, yaw, and yaw-rate, respectively, to reference values. The closed-loop dynamics (7)–(11) with the altitude control and yaw-rate control resemble Dubin's vehicle,[1] a well-studied model used in cooperative control.

III.A. Altitude Control

In this section, we design a main-rotor control, F_1, that stabilizes the helicopter altitude z to a desired value, z_d. The vertical acceleration in (11) is decoupled from the other equations of motion. Therefore, we consider the design of the altitude control separately from subsequent control designs.

Consider the quadratic potential

$$V(z) = \frac{1}{2}(z - z_d)^2 + \frac{1}{2}\dot{z}^2. \quad (12)$$

The time-derivative of V along solutions of (11) is

$$\dot{V} = (z - z_d)\dot{z} + \dot{z}\left(\frac{1}{m}F_1\cos\alpha - g\right). \quad (13)$$

Choosing the control

$$F_1 = \frac{m}{\cos\alpha}(g - z + z_d - k_1\dot{z}), \quad (14)$$

where $k_1 > 0$ is the altitude-control gain, yields

$$\dot{V} = -k_1\dot{z}^2 \leq 0. \quad (15)$$

We obtain the following result courtesy of Lyapunov's direct method.

Proposition 1 *Solutions to the idealized rotorcraft model (7)–(11) with F_1 given by (14) and arbitrary F_2 asymptotically converge to the set of trajectories for which $z = z_d$, where z_d a the reference altitude.*

Proposition 1 shows that we can use the main-rotor control (14) to stabilize the helicopter to a reference altitude independently of the choice of the tail-rotor control. Note that exact implementation of the altitude control requires knowledge of m, $\cos\alpha$, and g. We can achieve an approximate implementation of the control (14) using a PID controller. Letting $e = z_d - z$, then (14) has the form

$$F_1 = K_P e + K_I + K_D e, \tag{16}$$

where K_P, K_I, and K_D are (constant) gains. If K_I is multiplied by the integral of e, then the PID control (16) can be implemented without prior knowledge of any of the helicopter's properties.

III.B. Yaw Control

In this section we design a tail-rotor control, F_1, to steer the helicopter yaw θ to a (fixed) reference orientation, θ_d. Note that yaw-angle dynamics in (10) are uncoupled from the dynamics of the other state variables. Consider the potential function

$$U(\theta) = 1 - \cos(\theta_d - \theta) + \frac{1}{2}\dot{\theta}^2, \tag{17}$$

which is minimum when $\theta = \theta_d$ and $\dot{\theta} = 0$. The time-derivative of U along trajectories of (10) is

$$\dot{U} = -\sin(\theta_d - \theta)\dot{\theta} + \frac{l}{I}\dot{\theta}F_2. \tag{18}$$

Choosing the tail-rotor control

$$F_2 = \frac{I}{l}\left(\sin(\theta_d - \theta) - k_2\dot{\theta}\right), \tag{19}$$

where $k_2 > 0$ is a yaw-control gain, yields $\dot{U} = -k_2\dot{\theta}^2 \leq 0$. Although exact implementation of this control requires knowledge of I/l, it can be approximated by a PD controller that does not require such knowledge. We have the following result.

Proposition 2 *Solutions to the idealized rotorcraft model (7)–(11) with F_2 given by (19) and arbitrary F_1 asymptotically converge to the set of trajectories for which $\theta = \theta_d$, where θ_d is a (fixed) reference orientation.*

Next we analyze the behavior of the horizontal component of the inertial velocity under the combined action of the altitude and yaw controls. When the helicopter has reached the desired altitude, the steady-state altitude control is

$$F_1 = \frac{mg}{\cos\alpha} \triangleq \bar{F}_1. \tag{20}$$

Consequently, when the helicopter flies at constant altitude, (8) becomes

$$\dot{v} = \frac{1}{m}(\bar{F}_1 \sin\alpha\cos\beta + F_2\sin\beta - \gamma v^2). \tag{21}$$

Observe that, as the yaw control converges, F_2 tends to zero. And, as we describe below, the crab angle β tends to zero as well. In the limit $F_2 \to 0$ and $\beta \to 0$, (21) becomes

$$\dot{v} = \frac{1}{m}(\bar{F}_1 \sin\alpha - \gamma v^2) + \mathcal{O}(|F_2\sin\beta|) + \mathcal{O}(\beta^2). \tag{22}$$

Ignoring terms of order $\mathcal{O}(|F_2\sin\beta|)$ and $\mathcal{O}(\beta^2)$ suggests that (22) has an asymptotically stable equilibrium

$$v = \sqrt{\frac{\bar{F}_1\sin\alpha}{\gamma}} \triangleq v_0. \tag{23}$$

(There is also an unstable equilibrium at $-v_0$.) This analysis implies that the altitude control (14) also produces a constant horizontal speed.

The following analysis indicates that the helicopter direction of motion also converges to a constant—the reference orientation. Substituting (19) into (9) and using the definition of the crab angle, β, yields

$$\begin{aligned}\dot{\beta} &= \dot{\theta} - \frac{1}{mv}\left(F_1\sin\alpha\sin\beta - \frac{I}{l}\sin(\theta_d - \theta)\cos\beta - \frac{k_2 I}{l}\dot{\theta}\cos\beta\right) \\ &= \left(1 + \frac{k_2 I\cos\beta}{lmv}\right)\dot{\theta} - \frac{F_1\sin\alpha\sin\beta}{mv} + \frac{k_2 I}{lmv}\sin(\theta_d - \theta)\cos\beta.\end{aligned} \tag{24}$$

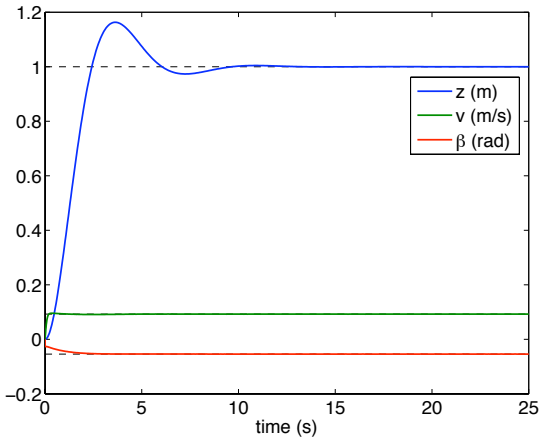

(a) Altitude and Yaw-rate Control Simulation

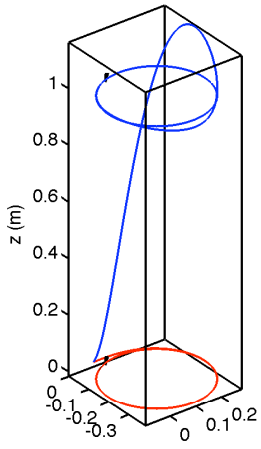

(b) Simulated Helicopter 3D Trajectory

Figure 3. Numerical simulation of closed-loop helicopter model with altitude control and yaw-rate control. (a) The simulated solution converges to the reference altitude ($z_d = 1$) and to the predicted horizontal speed and crab angle ($v_0 = 0.09$ m/s and $\beta_0 = -0.05$ rad). (b) The 3D trajectory (blue line) of the helicopter converges to a horizontally oriented circle at $z = 1$. (The red line represents a 2D projection of the helicopter's trajectory onto a horizontal plane.)

At the desired altitude and desired yaw angle, (24) becomes

$$\dot{\beta} = -\frac{\bar{F}_1 \sin\alpha \sin\beta}{m v_0}, \tag{25}$$

which has an asymptotically stable equilibrium at $\beta = 0$ (and an unstable equilibrium at $\beta = \pi$). This analysis suggests that the combination of altitude control and yaw control drive the helicopter along an inertial bearing equal to the desired heading. That is, the steady-state crab angle is zero. These conclusions are supported by numerical simulations.

III.C. Yaw-Rate Control and Stabilization of Collective Motion

Rather than driving the helicopter to a desired yaw angle, we now consider driving the helicopter to a constant yaw *rate*, u. Consider the quadratic potential

$$S(\theta) = \frac{1}{2}(\dot{\theta} - u)^2. \tag{26}$$

Along solutions of (10), the time-derivative of S is

$$\dot{S} = (\dot{\theta} - u)\frac{l}{I}F_2. \tag{27}$$

Choosing the control

$$F_2 = -\frac{k_2 I}{l}(\dot{\theta} - u) \tag{28}$$

yields $\dot{S} = -k_2(\dot{\theta} - u)^2 \leq 0$. This result implies that the yaw-rate control (28) drives the helicopter to a desired turning rate, $\dot{\theta} = u$.

Substituting (28) into (9), using the definition of β, and evaluating the result at a constant altitude and a constant yaw rate yields

$$\begin{aligned} \dot{\beta} &= \dot{\theta} - \frac{1}{mv}\left(F_1 \sin\alpha \sin\beta - \frac{k_2 I}{l}(\dot{\theta} - u)\cos\beta\right) \\ &= u - \frac{\bar{F}_1 \sin\alpha}{m v_0}\sin\beta \end{aligned} \tag{29}$$

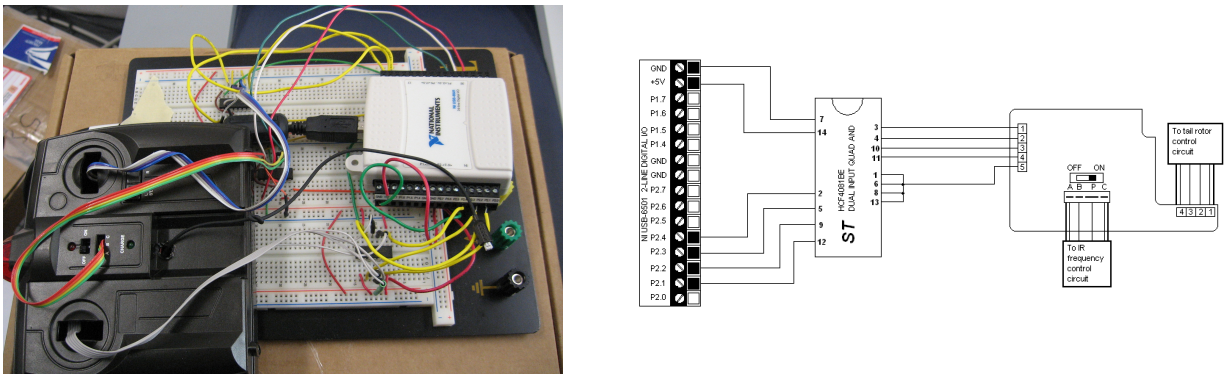

(a) Transmitter interface electronics

(b) Main-rotor control circuit

Figure 4. The transmitter interface electronics enables a PC running LabVIEW to control the main rotor and tail rotor of three helicopters. The interface electronics include a PicooZ IR transmitter, a National Instruments USB digital I/O board, and a Dual Input Quad AND chip.

Provided $\frac{\bar{F}_1 \sin\alpha}{mv_0} \geq u$, then (29) has an asymptotically stable equilibrium at $\beta = \sin^{-1}\left(\frac{muv_0}{F_1 \sin\alpha}\right) \triangleq \beta_0$. That is, the helicopter turns at the desired yaw rate and has a constant crab angle, β_0, which implies $\dot{\psi} = u$.

Figure 3 contains a numerical simulation of (7)–(11) with F_1 given by (14) and F_2 by (28). The simulation parameters are $\alpha = 5°$, $\gamma = 1$, $m = 0.01$ kg, $l = 0.1$ m, $I = ml^2/2$, $g = 9.81$ m/s/s, $z_d = 1$, $k_1 = k_2 = 1$, and $u = -1$. The simulated trajectory indeed converges to the reference altitude, $z_d = 1$, and a constant speed, $v_0 = 0.09$ m/s, while tracing a horizontally oriented circle at a constant turning rate. (The radius of the circle is v_0/u, where $u = -1$ for this example.) Furthermore, the crab angle converges to $\beta_0 = -0.05$ rad. This analysis leads to the following proposition.

Proposition 3 *The horizontal dynamics of the closed-loop model (7)–(11) with altitude control (14) and yaw-rate control (28) asymptotically converges to the dynamics of a planar self-propelled particle,*

$$\begin{aligned} \dot{r} &= v_0 e^{i\psi} \\ \dot{\psi} &= u, \end{aligned} \tag{30}$$

where r is position, v_0 is speed, ψ is direction of motion, and u is the reference yaw-rate.

The main advantage of obtaining closed-loop dynamics having the form (30) is the existence of a rich library of decentralized algorithms to cooperatively control systems of self-propelled particles.[4,7–11] In this formulation the yaw-rate control tracks the reference input u, to be generated by a cooperative control law.

IV. Experimental Results

We conducted experimental flight tests of a PicooZ micro-helicopter in the U. Maryland VICON Motion Capture Facility. We performed automated closed-loop control of a PicooZ helicopter using sensory feedback from a motion-capture system and PC-based actuation via an infrared transmitter. We designed the transmitter interface electronics shown in Figure 4 to enable a laptop computer running LabVIEW to control the main rotor and tail rotor of three PicooZ helicopters. The control PC receives the motion-capture data in real-time over a TCP/IP connection with the VICON server. Each helicopter is equipped with a set of reflective markers used by the motion-capture system. (The markers are visible in Figure 1(a).)

The flight tests described here pertain to altitude control of a single helicopter. We implemented in LabVIEW a PID altitude control of the form (16) with a dynamic integral term. The control launches the helicopter and stabilizes its altitude to a desired value. Figure 5 shows results from a forty-second experiment with a desired altitude of 1 m. For this experiment, the proportional gain was 0.004 and the integral gain was 0.0000012. The derivative gain was set to zero because of noisy measurements. The controller achieves a short rise time and attenuates oscillations to an amplitude less than 0.2 m. In ongoing work we are developing a low-pass filter for the altitude measurements that will enable us to damp out altitude oscillations by adding derivative control.

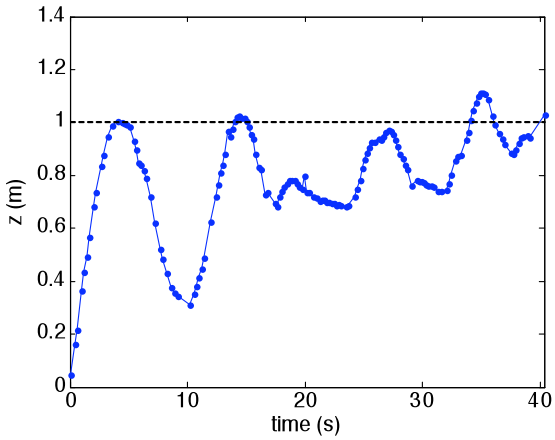

(a) Altitude Control Experimental Results

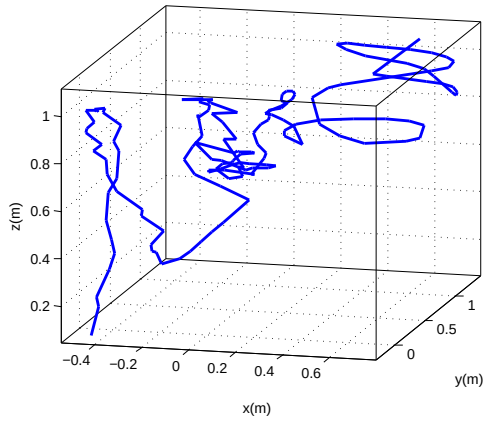

(b) Experimental Helicopter 3D Trajectory

Figure 5. Experimental results for altitude control of a single helicopter using motion-capture feedback. (a) The controller achieves a short rise time to the desired height of 1 m and attenuates oscillations to an amplitude less than 0.2 m. (b) The 3D trajectory of the helicopter under altitude control.

V. Conclusion

This paper describes an idealized 3D model of a micro-helicopter and several feedback control algorithms for this model. The closed-loop dynamics of the helicopter model resemble Dubin's vehicle—a simple vehicle model for which a plethora of cooperative control algorithms exist. Cooperative behavior of multiple micro-helicopters is now possible through the combined behavior of presently available cooperative control algorithms and the state feedback control algorithms described here.

In ongoing work, we are further developing our micro-helicopter cooperative behavior testbed. The testbed utilizes the U. Maryland Motion Capture Facility to perform (offboard) state feedback control of multiple RC helicopters.[2,12] The testbed will support the design and demonstration of autonomous capabilities including improved gust tolerance[5,6] and visual servoing.[3]

Acknowledgments

We thank Dr. Sean Humbert for generously granting access to the VICON Motion Capture Facility in the Autonomous Vehicle Laboratory at the University of Maryland. We also thank Joseph Conroy for assisting with the VICON experiments.

References

[1]L. E. Dubins. On curves of minimal length with a constraint on average curvature, and with prescribed initial and terminal positions and tangents. *Amer. J. Mathematics*, 79(3):497–517, 1957.

[2]C. Haosheng and C. Darong. Identification of a model helicopter's yaw dynamics. *J. Dynamic Systems, Measurement, and Control*, 127(1):140–145, 2005.

[3]J. S. Humbert, R. M. Murray, and M. H. Dickinson. Pitch-altitude control and terrain following based on bio-inspired visuomotor convergence. In *Proc. AIAA Guidance, Navigation and Control Conf. and Exhibit (electronic)*, San Francisco, California, August 2005.

[4]E. W. Justh and P. S. Krishnaprasad. Equilibria and steering laws for planar formations. *Systems and Control Letters*, 52(1):25–38, 2004.

[5]D. A. Paley. Cooperative control of an autonomous sampling network in an external flow field. Submitted to *47th IEEE Conf. Decision and Control*, invited session on "Autonomous exploration and remote sensing".

[6]D. A. Paley. Stabilization of collective motion in a uniform and constant flow field. *2008 AIAA Guidance, Navigation and Control Conf. and Exhibit*, accepted.

[7]D. A. Paley, N. E. Leonard, and R. Sepulchre. Stabilization of symmetric formations to motion around convex loops.

Systems and Control Letters, 57(3):209–215, 2008.

[8]K. Savla, F. Bullo, and E. Frazzoli. The coverage problem for loitering Dubins vehicles. In *Proc. 46th IEEE Conf. Decision and Control*, pages 1398–1403, New Orleans, Louisiana, December 2007.

[9]K. Savla, E. Frazzoli, and F. Bullo. On the point-to-point and traveling salesperson problems for Dubin's vehicle. In *Proc. 2005 Amer. Control Conf.*, pages 786–791, Portland, Oregon, June 2005.

[10]R. Sepulchre, D. A. Paley, and N. E. Leonard. Stabilization of planar collective motion: All-to-all communication. *IEEE Trans. Automatic Control*, 52(5):811–824, 2007.

[11]R. Sepulchre, D. A. Paley, and N. E. Leonard. Stabilization of planar collective motion with limited communication. *IEEE Trans. Automatic Control*, 53(3):706–719, 2008.

[12]C. Tisse, T. Fauvel, and H. Durrant-Whyte. A micro aerial vehicle motion capture system. In *Proc. 1st Int. Conf. on Sensing Technology*, pages 533–530, Palmerston North, New Zealand, November 2005.